# Control Design for Position Synchronization in Central Converter Multi-Machine Actuators

**Cláudio Lima and Prof. James Cale**

Colorado State University

19 July 2023

1. Motivation
2. $\mathcal{H}_\infty$ Control Design Method
3. Model Linearization
4. $\mathcal{H}_\infty$ Method Applied to the Linearized Model
5. Controller Performance
6. Conclusions

# Motivation

**More Electric Aircraft (MEA)**

The trend towards More Electric Aircraft (MEA) is expected to revolutionize the aerospace industry in coming years.

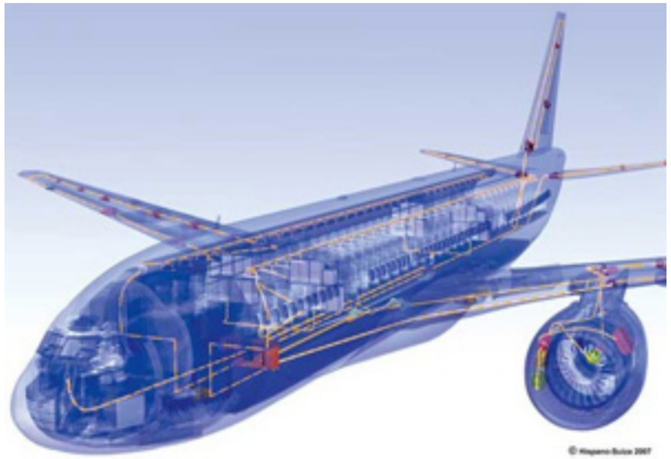

Potential Advantages:

- Reduced maintenance
- Elimination of hydraulic fluids
- Lighter weight and lower fuel burn
- Enhanced system control and diagnostics
- Fault-tolerant power electronic structures

## Thrust Reverse Actuation System (TRAS)

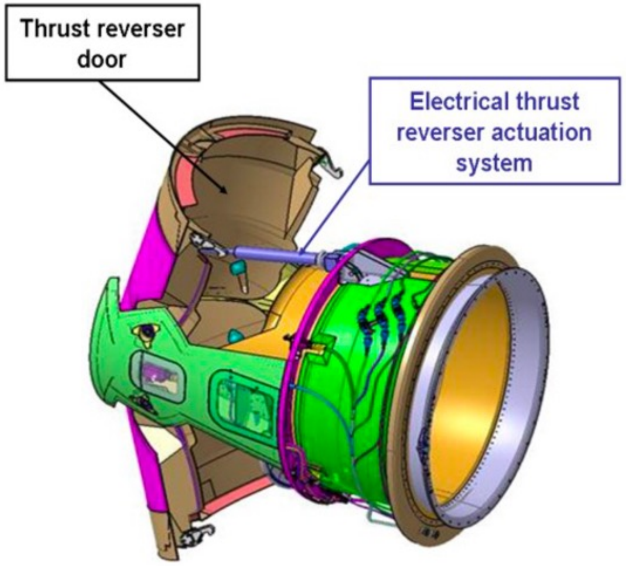


Figure 1: 3-D view of a TRAS (from [1]).

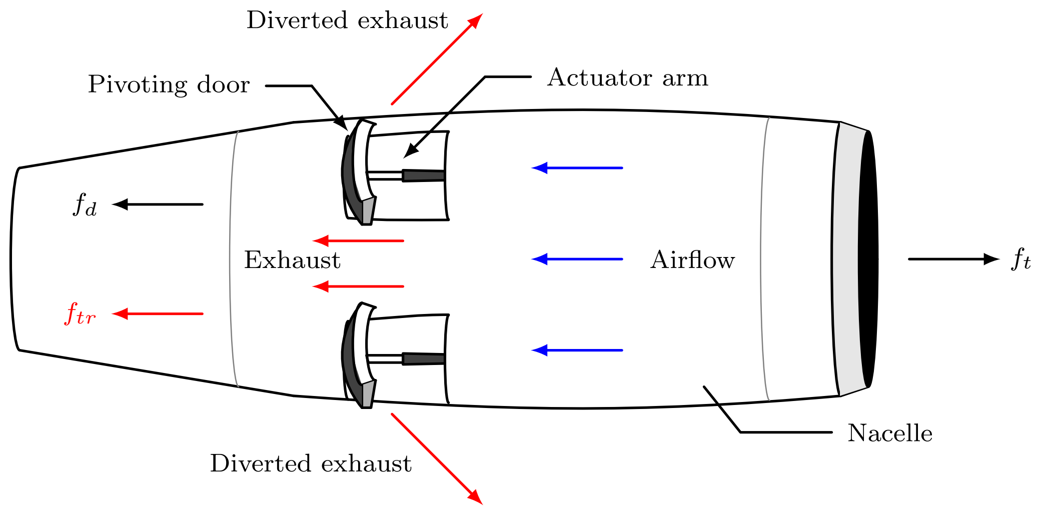


Figure 2: Notional illustration of pivoting-door TRAS [2].

**Electromechanical Thrust Reverse Actuation System (EM-TRAS) Architectures**

1. Distributed converter multiple-motor (DCMM)
2. Central converter multiple-motor (CCMM)

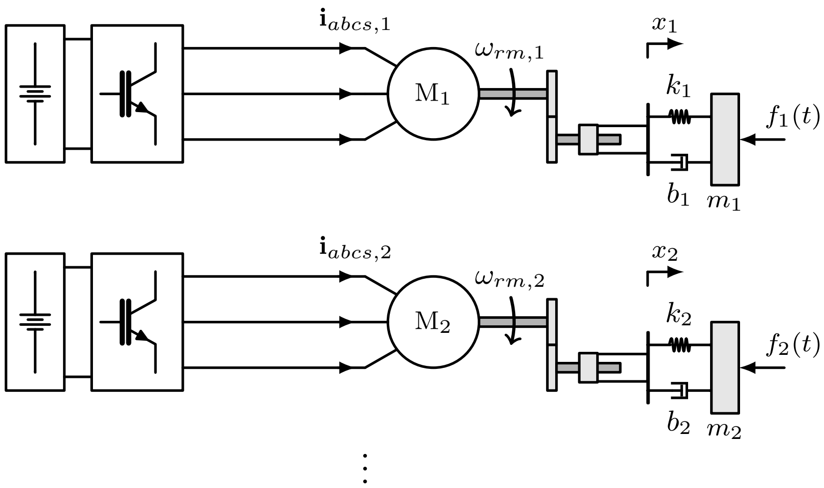


Figure 3: DCMM architecture.

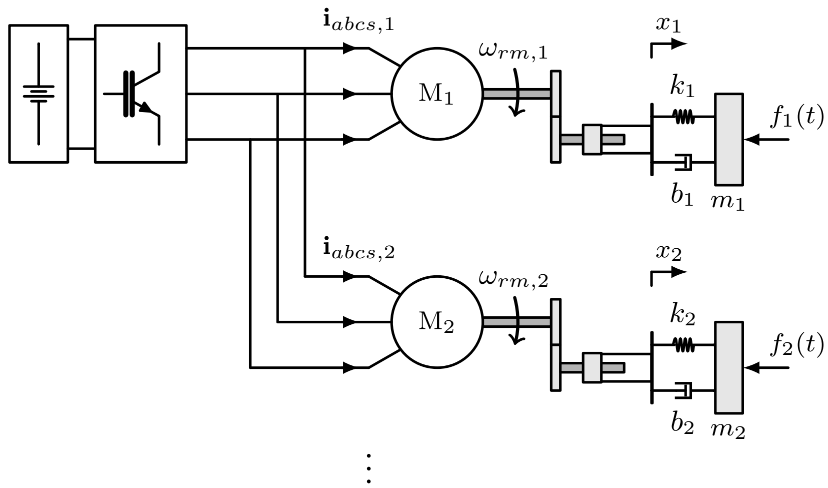


Figure 4: CCMM architecture.

**Choice of Architectures**

- The DCMM architecture with permanent magnet synchronous machines would likely be the "easiest" choice.
  - But larger cost of high-power electronic drives
  - Supply chain risk for large rare Earth magnets
- The CCMM architecture with induction machines (IMs) is a lower cost option

**CCMM Architecture Challenge**

Constraints:

1. Generally unbalanced load torque from unsymmetrical wind forces
2. Require both speed and position synchronization (within 1 revolution)
3. Common three-phase voltage source

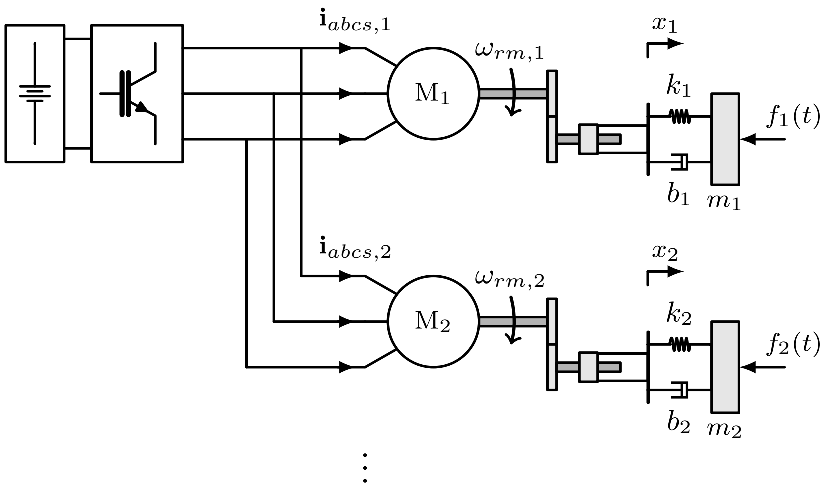


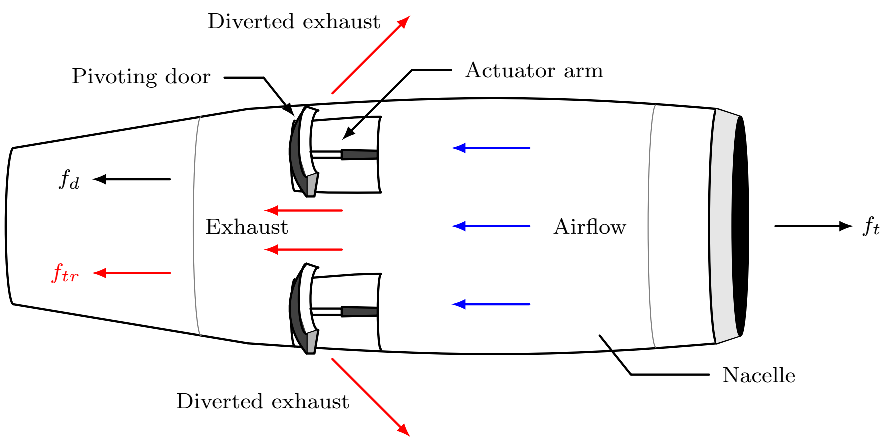

**Rotor Position Synchronization Solution**

Low-power three-phase external variable resistor in series with each induction motor

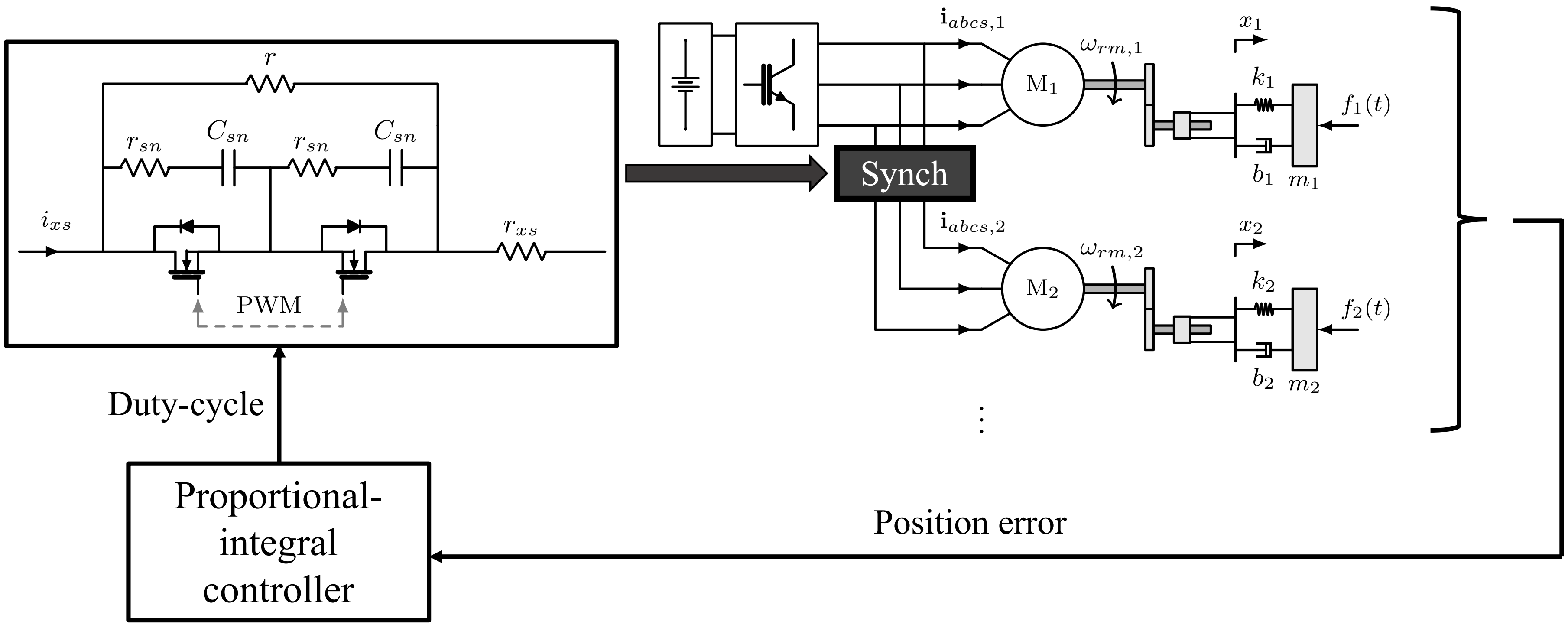


Figure 5: Position synchronization method [2].

**Goal**:

- Optimal control design applied to rotor position synchronization in the CCMM for optimal tracking of relative rotor position errors

**Key contributions**:

- Solution of the optimal control synthesis problem for achieving rotor position synchronization in a set of parallel IMs with unequal torque loads, within a CCMM architecture.
  - Optimization to minimize position error and settling time
- Description of the IM linearization process and weighting function selections for the modified plant model.
- Validation of the approach and comparison to previous results using detailed numerical case studies, with voltage- and current-based CCMM primary control strategies.

# $\mathcal{H}_\infty$ Control Design Method

# $\mathcal{H}_\infty$ Control Design Method

## Description of the Control Synthesis Problem

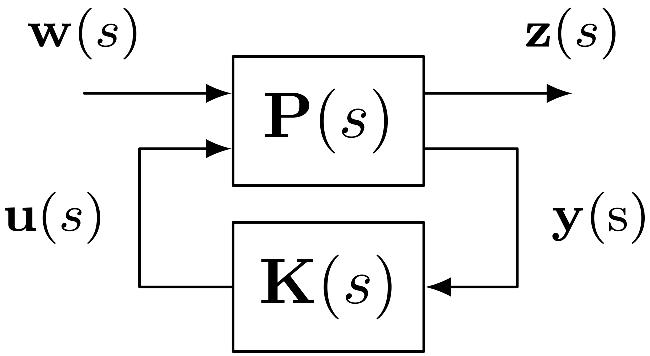


$$\mathbf{z} = F_l(\mathbf{P}, \mathbf{K})\mathbf{w}$$

$$F_l(\mathbf{P}, \mathbf{K}) := P_{11} + P_{12}\mathbf{K}(\mathbf{I} - P_{22}\mathbf{K})^{-1} P_{21}$$

$$\mathbf{K} = \arg\min_{\mathbf{K} \in \mathcal{K}} ||F_l(\mathbf{P}, \mathbf{K})||_\infty$$

$$\begin{bmatrix} \mathbf{z}(s) \\ \mathbf{y}(s) \end{bmatrix} = \mathbf{P}(s) \begin{bmatrix} \mathbf{w}(s) \\ \mathbf{u}(s) \end{bmatrix} = \begin{bmatrix} P_{11}(s) & P_{12}(s) \\ P_{21}(s) & P_{22}(s) \end{bmatrix} \begin{bmatrix} \mathbf{w}(s) \\ \mathbf{u}(s) \end{bmatrix}$$

$$\mathbf{u}(s) = \mathbf{K}(s)\mathbf{y}(s)$$

$$||F_l(\mathbf{P}, \mathbf{K})||_\infty = \max_{\mathbf{w}(t) \neq 0} \frac{||\mathbf{z}(t)||_2}{||\mathbf{w}(t)||_2}$$

**Importance Weights**

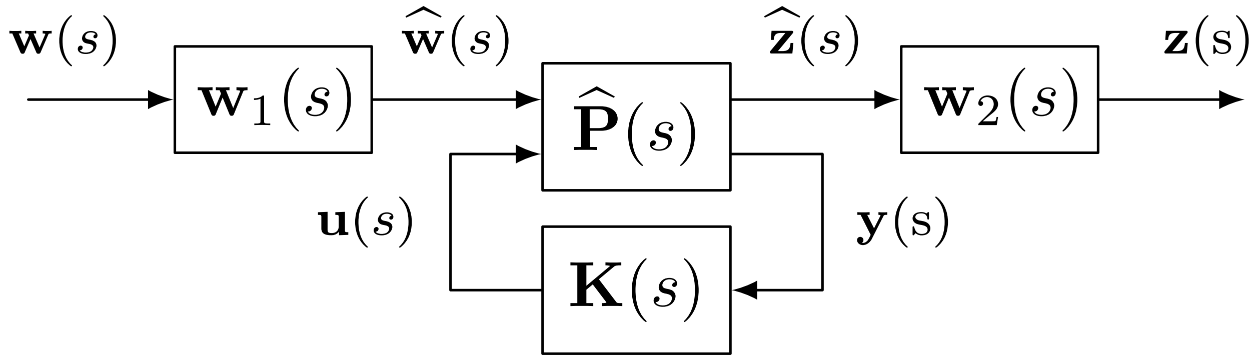


$$\widehat{\mathbf{P}}(s) := \begin{bmatrix} \widehat{P}_{11}(s) & \widehat{P}_{12}(s) \\ \widehat{P}_{11}(s) & \widehat{P}_{22}(s) \end{bmatrix}$$

$$\mathbf{P}(s) = \begin{bmatrix} \mathbf{w}_2(s)\widehat{P}_{11}(s)\mathbf{w}_1(s) & \mathbf{w}_2(s)\widehat{P}_{12}(s) \\ \widehat{P}_{11}(s)\mathbf{w}_1(s) & \widehat{P}_{22}(s) \end{bmatrix}$$

# Model Linearization

**Induction Machine Standard Equations**

$$v_{qs} = r_s i_{qs} + \omega\lambda_{ds} + p\lambda_{qs}$$
$$v_{ds} = r_s i_{ds} - \omega\lambda_{qs} + p\lambda_{ds}$$
$$v_{qr} = r_r i_{qr} + (\omega - \omega_r)\lambda_{dr} + p\lambda_{qr}$$
$$v_{dr} = r_r i_{dr} - (\omega - \omega_r)\lambda_{qr} + p\lambda_{dr}$$

$$\lambda_{qs} = L_{ls} i_{qs} + L_m(i_{qs} + i_{qr})$$
$$\lambda_{ds} = L_{ls} i_{ds} + L_m(i_{ds} + i_{dr})$$
$$\lambda_{qr} = L_{lr} i_{qr} + L_m(i_{qs} + i_{qr})$$
$$\lambda_{dr} = L_{lr} i_{dr} + L_m(i_{ds} + i_{dr})$$

$$T_e = \frac{3}{2}\frac{P}{2}\frac{L_m}{\sigma L_s L_r}(\lambda_{qs}\lambda_{dr} - \lambda_{ds}\lambda_{qr})$$

$$T_e - T_L = Jp\omega_{rm} + B_m\omega_{rm}$$

**Transformed Equations in Synchronous Reference Frame**

$$v_{qs}^e = (\mu_s + p)\lambda_{qs}^e + \omega_e \lambda_{ds}^e - \mu_s \frac{L_m}{L_r}\lambda_{qr}^e$$

$$0 = (\mu_s + p)\lambda_{ds}^e - \omega_e \lambda_{qs}^e - \mu_s \frac{L_m}{L_r}\lambda_{dr}^e$$

$$0 = (\mu_r + p)\lambda_{qr}^e + (\omega_e - \omega_r)\lambda_{dr}^e - \mu_r \frac{L_m}{L_s}\lambda_{qs}^e$$

$$0 = (\mu_r + p)\lambda_{dr}^e - (\omega_e - \omega_r)\lambda_{qr}^e - \mu_r \frac{L_m}{L_s}\lambda_{ds}^e$$

$$\mu_s := \frac{r_s}{(\sigma L_s)}$$

$$\mu_r := \frac{r_r}{(\sigma L_r)}$$

$$\sigma := 1 - \frac{L_m^2}{(L_s L_r)}$$

**Linearization Procedure**

Taylor expansion: DC component and small-signal component

$$f(t) = f_0 + \widetilde{f}(t)$$

$$\begin{aligned}\widetilde{v}^e_{qs} &= \left(\lambda^e_{qs0} - \frac{L_m}{L_r}\lambda^e_{qr0}\right)\widetilde{\mu}_s + (\mu_{s0} + p)\widetilde{\lambda}^e_{qs} \\ &\quad \omega_e\widetilde{\lambda}^e_{ds} - \mu_{s0}\frac{L_m}{L_r}\widetilde{\lambda}^e_{qr} \\ \widetilde{v}^e_{ds} &= \left(\lambda^e_{ds0} - \frac{L_m}{L_r}\lambda^e_{dr0}\right)\widetilde{\mu}_s + (\mu_{s0} + p)\widetilde{\lambda}^e_{ds} \\ &\quad -\omega_e\widetilde{\lambda}^e_{qs} - \mu_{s0}\frac{L_m}{L_r}\widetilde{\lambda}^e_{dr}\end{aligned}$$

$$\begin{aligned}\widetilde{v}^e_{qr} &= (\mu_r + p)\widetilde{\lambda}^e_{qr} - \lambda^e_{dr0}\widetilde{\omega}_r \\ &\quad +(\omega_e - \omega_{r0})\widetilde{\lambda}^e_{dr} - \mu_r\frac{L_m}{L_s}\widetilde{\lambda}^e_{qs} \\ \widetilde{v}^e_{dr} &= (\mu_r + p)\widetilde{\lambda}^e_{dr} + \lambda^e_{qr0}\widetilde{\omega}_r \\ &\quad -(\omega_e - \omega_{r0})\widetilde{\lambda}^e_{qr} - \mu_r\frac{L_m}{L_s}\widetilde{\lambda}^e_{ds} \\ \widetilde{T}_e &= K_T(\lambda^e_{dr0}\widetilde{\lambda}^e_{qs} + \lambda^e_{qs0}\widetilde{\lambda}^e_{dr} \\ &\quad -\lambda^e_{ds0}\widetilde{\lambda}^e_{ds} - \lambda^e_{qr0}\widetilde{\lambda}^e_{ds})\end{aligned}$$

## Resulting Linearized Model

State-space representation:

$$p\widetilde{\mathbf{x}} = \mathbf{A}\widetilde{\mathbf{x}} + \mathbf{B}\widetilde{\mathbf{u}}$$

$$\widetilde{\mathbf{x}} = \begin{bmatrix}\widetilde{\lambda}^e_{qs} & \widetilde{\lambda}^e_{ds} & \widetilde{\lambda}^e_{qr} & \widetilde{\lambda}^e_{dr} & \widetilde{\omega}_r & \widetilde{\theta}_r\end{bmatrix}^T$$

$$\widetilde{\mathbf{u}} = \begin{bmatrix}\widetilde{v}^e_{qs} & \widetilde{\mu}_s & \widetilde{T}_L\end{bmatrix}^T$$

$$\mathbf{A} = \begin{bmatrix} -\mu_{s0} & \omega_e & \frac{\mu_r L_m}{L_s} & 0 & \left(\frac{K_T}{J'}\right)\lambda^e_{dr0} & 0 \\ -\omega_e & -\mu_{s0} & 0 & \frac{\mu_r L_m}{L_s} & -\left(\frac{K_T}{J'}\right)\lambda^e_{qr0} & 0 \\ \frac{\mu_{s0} L_m}{L_r} & 0 & -\mu_r & s_0\omega_e & -\left(\frac{K_T}{J'}\right)\lambda^e_{ds0} & 0 \\ 0 & \frac{\mu_{s0} L_m}{L_r} & -s_0\omega_e & -\mu_r & \left(\frac{K_T}{J'}\right)\lambda^e_{qs0} & 0 \\ 0 & 0 & \lambda^e_{dr0} & -\lambda^e_{qr0} & -\frac{B'_m}{J'} & 1 \\ 0 & 0 & 0 & 0 & 0 & 0 \end{bmatrix}^T \quad \mathbf{B} = \begin{bmatrix} 1 & (L_m/L_r)\lambda^e_{qr0} - \lambda^e_{qs0} & 0 \\ 0 & (L_m/L_r)\lambda^e_{dr0} - \lambda^e_{ds0} & 0 \\ 0 & 0 & 0 \\ 0 & 0 & 0 \\ 0 & 0 & -1/J' \\ 0 & 0 & 0 \end{bmatrix}$$

**Validation**

- Step change in load torque (1 to 0.8 pu)
- Compare linear (solid line) and complete (dashed line) models' responses

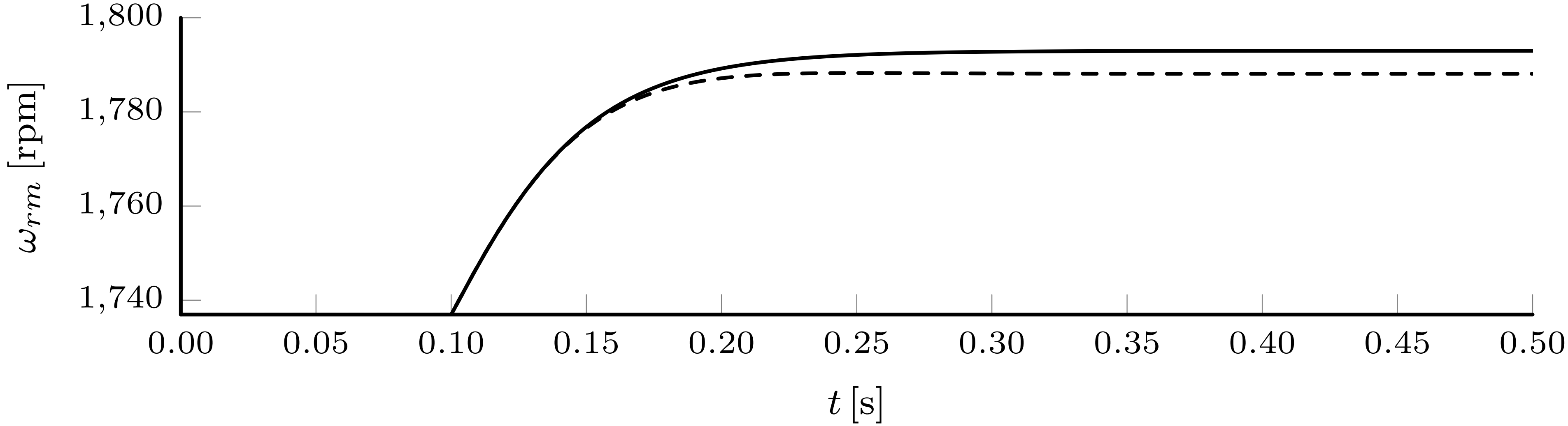


Figure 6: Rotor speed.

**Validation**

- Step change in load torque (1 to 0.8 pu)
- Compare linear (solid line) and complete (dashed line) models' responses

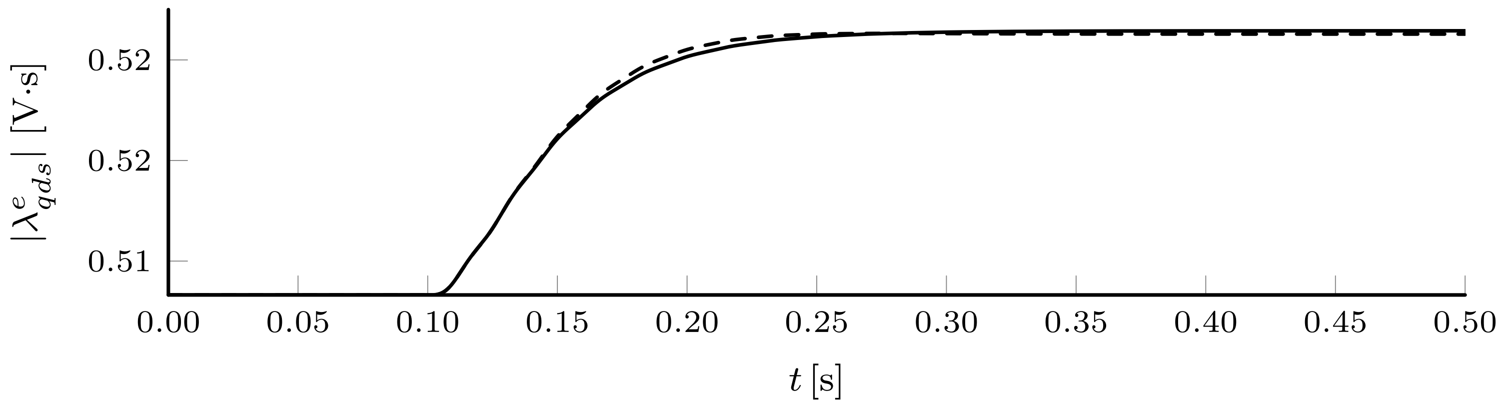


Figure 7: Stator fluxes.

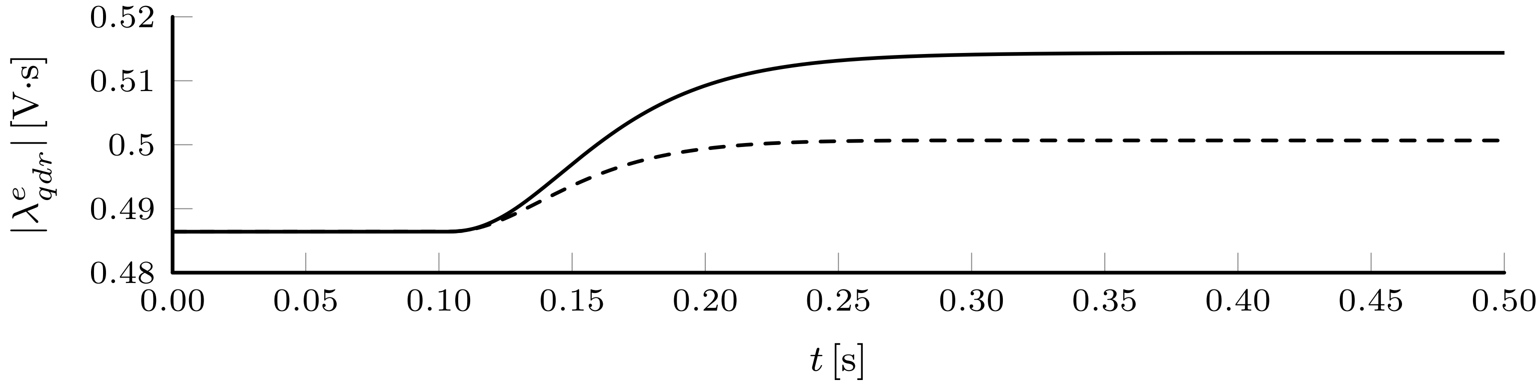


Figure 8: Rotor fluxes.

**Validation**

- Step change in external resistance (0 to 4 pu)
- Compare linear (solid line) and complete (dashed line) models' responses

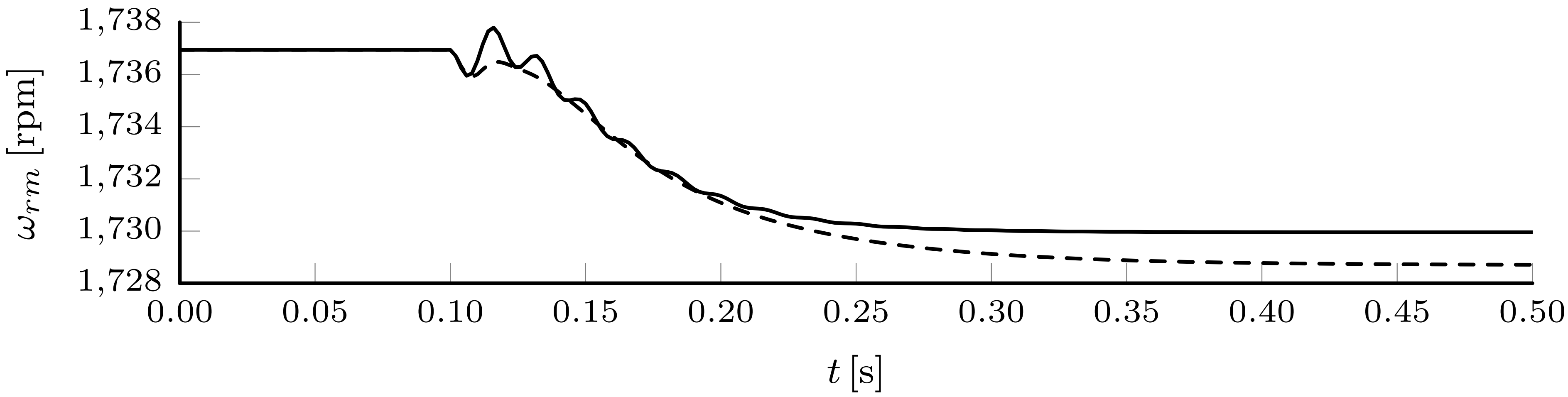


Figure 9: Rotor speed.

**Validation**

- Step change in external resistance (0 to 4 pu)
- Compare linear (solid line) and complete (dashed line) models' responses

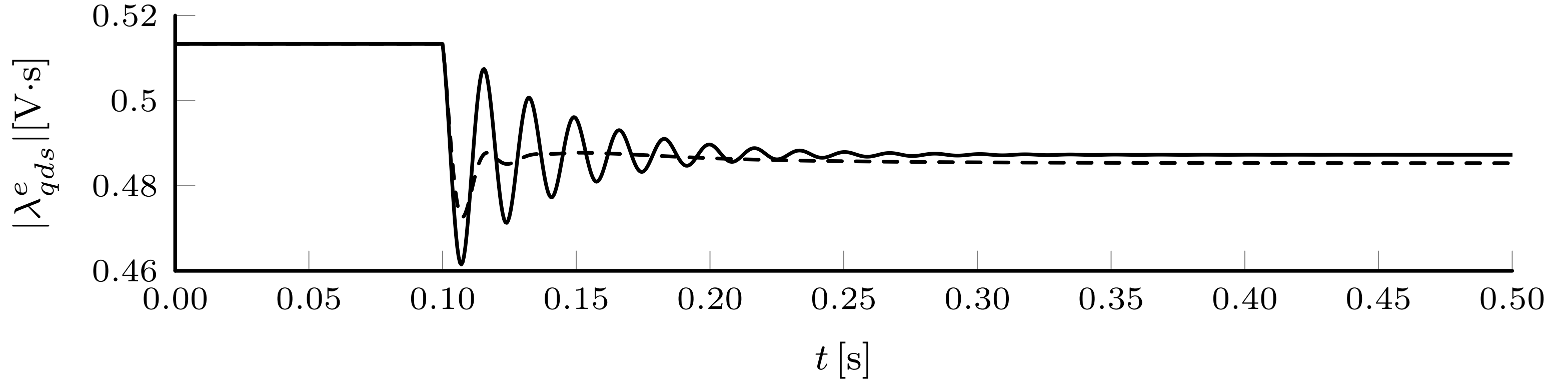


Figure 10: Stator fluxes.

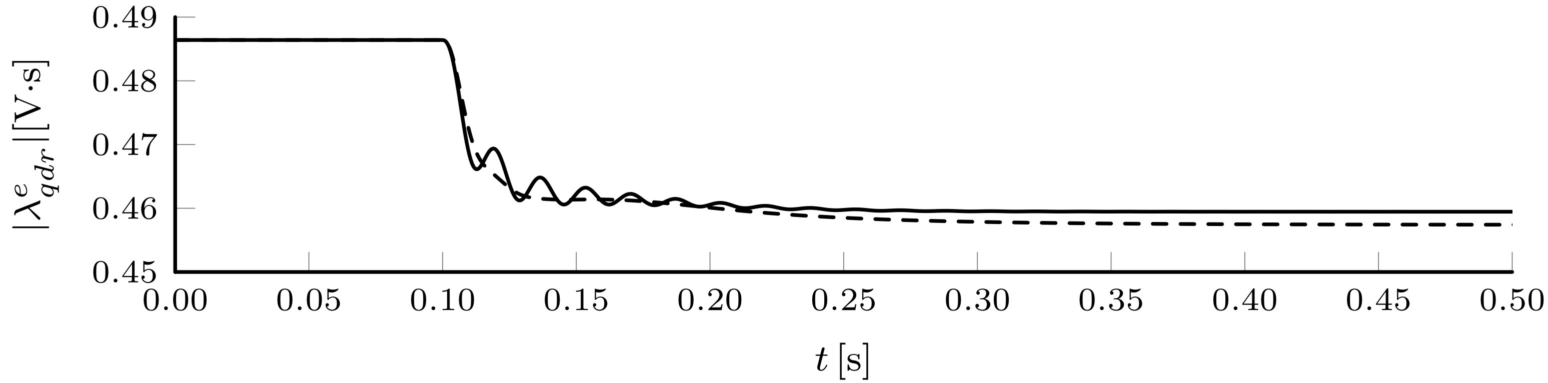


Figure 11: Rotor fluxes.

# $\mathcal{H}_\infty$ Method Applied to the Linearized Model

**Definition of the vector signals**

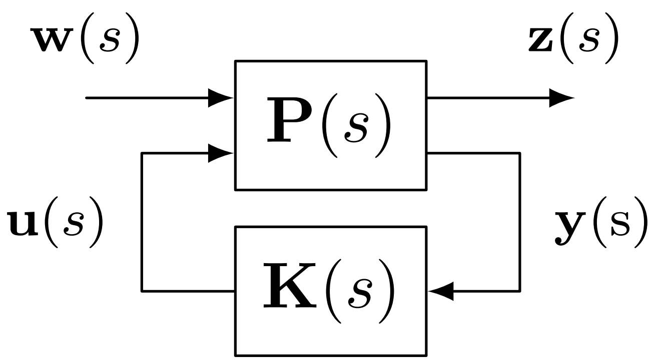


$$\mathbf{w} := \begin{bmatrix} \widetilde{T}_{L,1} & \widetilde{T}_{L,1} & \widetilde{n} \end{bmatrix}^T$$

$$\mathbf{z} := \begin{bmatrix} \delta\widetilde{\theta}_{rm} & \widetilde{\mu}_{s,2} \end{bmatrix}^T$$

$$\mathbf{y} := \begin{bmatrix} \delta\widetilde{\theta}_{rm} + \widetilde{n} \end{bmatrix}$$

$$\mathbf{u} := \begin{bmatrix} \widetilde{\mu}_{s,2} \end{bmatrix}$$

**Definition of the importance weights**

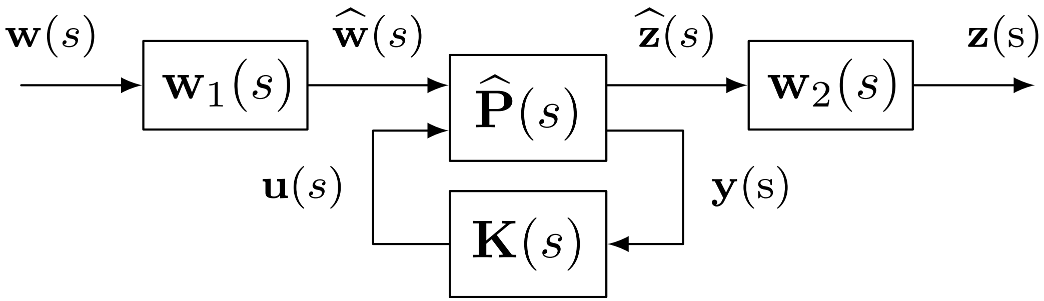


$$\mathbf{w}_1 = \begin{bmatrix} w_{1,1} & w_{1,2} & w_{1,3} \end{bmatrix} = \begin{bmatrix} 0.16 & 0.16 & 5.73\times10^{-6} \end{bmatrix}$$

- Weights applied to the load torques and measurement noise.

$$\mathbf{w}_2 = \begin{bmatrix} w_{2,1} & w_{2,2} \end{bmatrix} = \begin{bmatrix} \frac{100}{s+0.1} & \frac{0.2s}{s+6283} \end{bmatrix}$$

- Weights applied to the position error (controlled signal) and external resistance (manipulated signal).
- Position error weight: integrator (0.1 rad/s cut-off frequency and 1,000 DC gain).
- External resistance: limits the actuation bandwidth to 1,000 Hz.

# Controller Performance

**Simulation setup**

- Three 15 hp induction machines, single central power converter, resistor control boards
- Central converter primary control
  - Compensated Volts-per-Hertz - CVHz (open loop)
  - Indirect oriented-field control - IDFOC (closed loop)
- Unbalanced load conditions
  - $T_{L,1} = 1.0\,\text{pu}$, $T_{L,2} = 0.8\,\text{pu}$, and $T_{L,3} = 0.7\,\text{pu}$
- MATLAB® version R2022b.

## Compensated Volts-per-Hertz

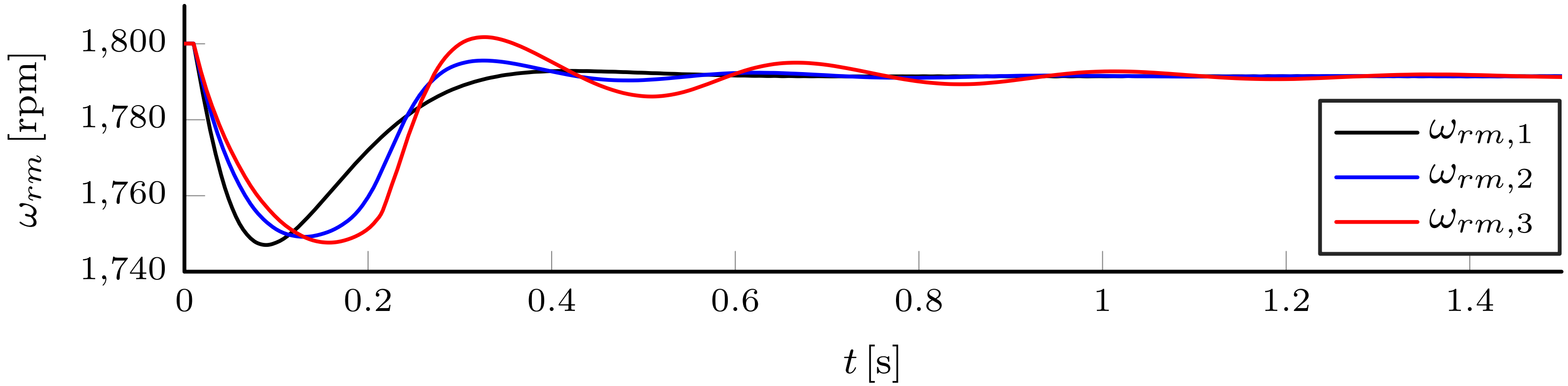


Figure 12: Rotor speeds.

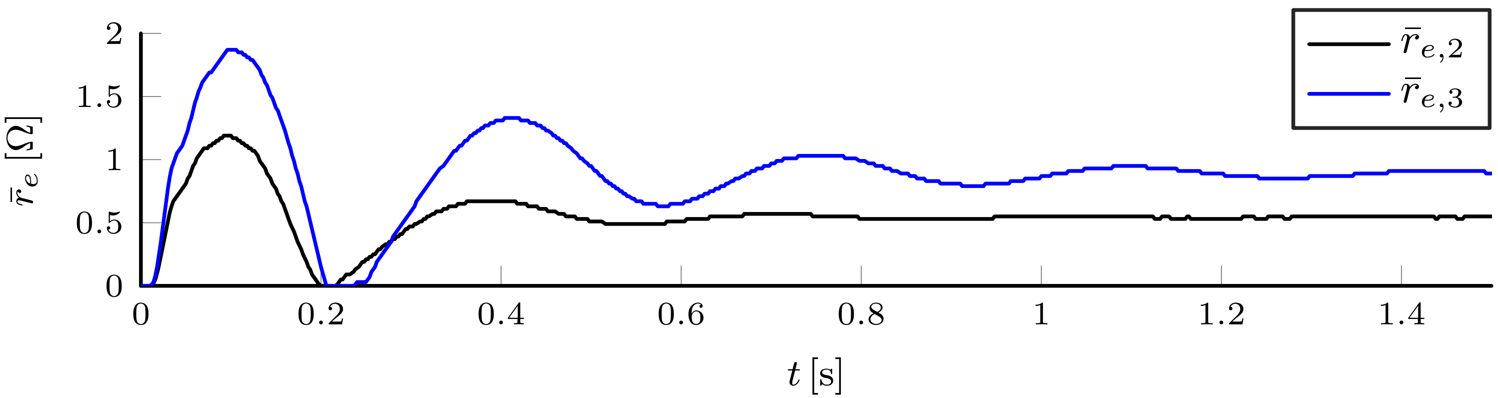


Figure 13: External resistances.

**Compensated Volts-per-Hertz**

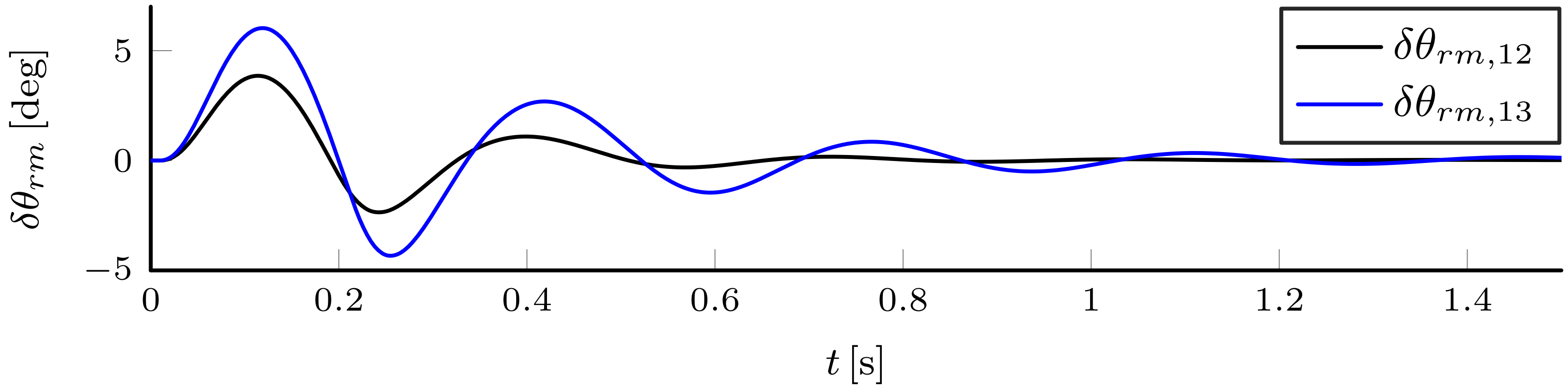


Figure 14: Rotor position errors.

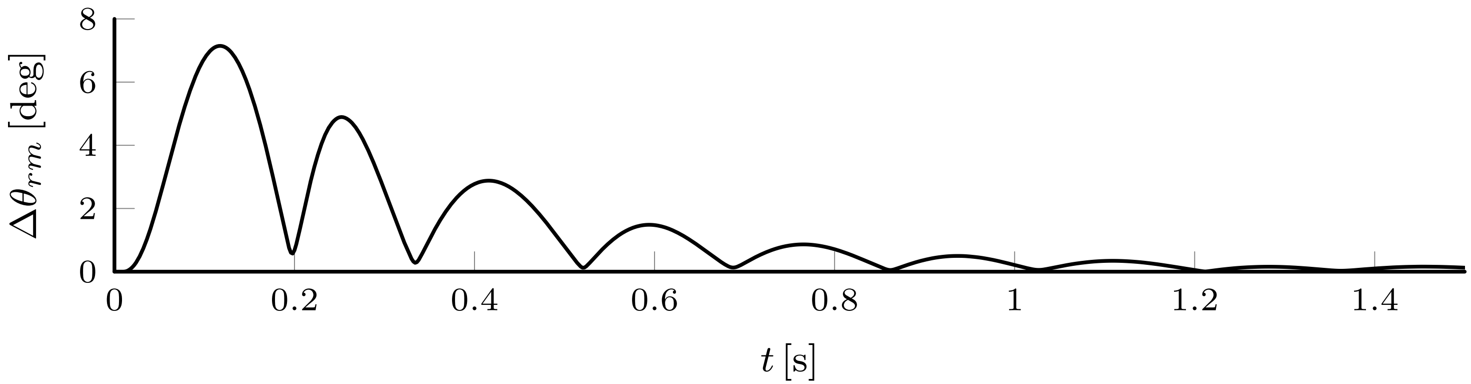


Figure 15: Normed position error.

## Indirect Field-Oriented Control

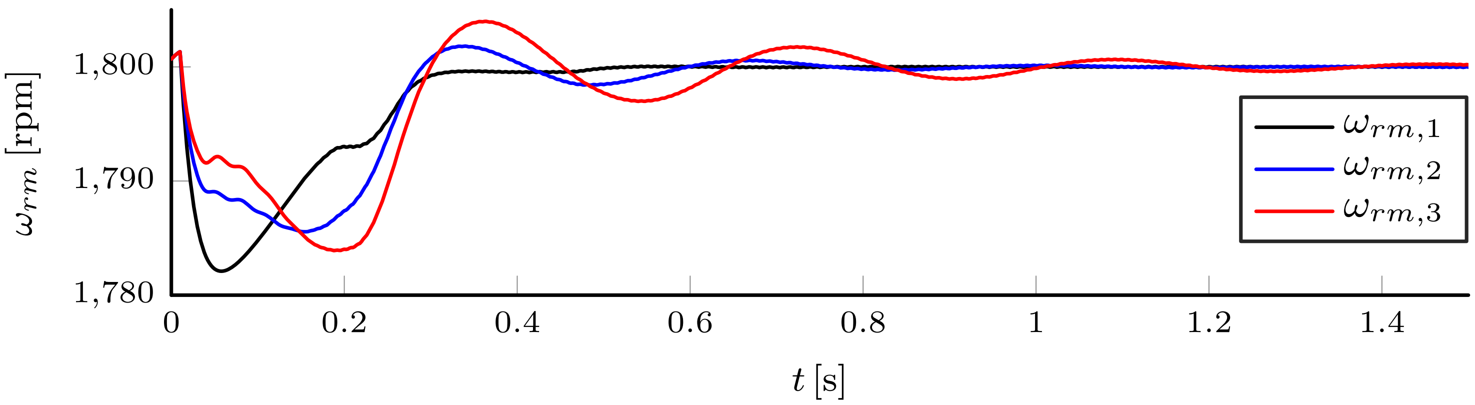


Figure 16: Rotor speeds.

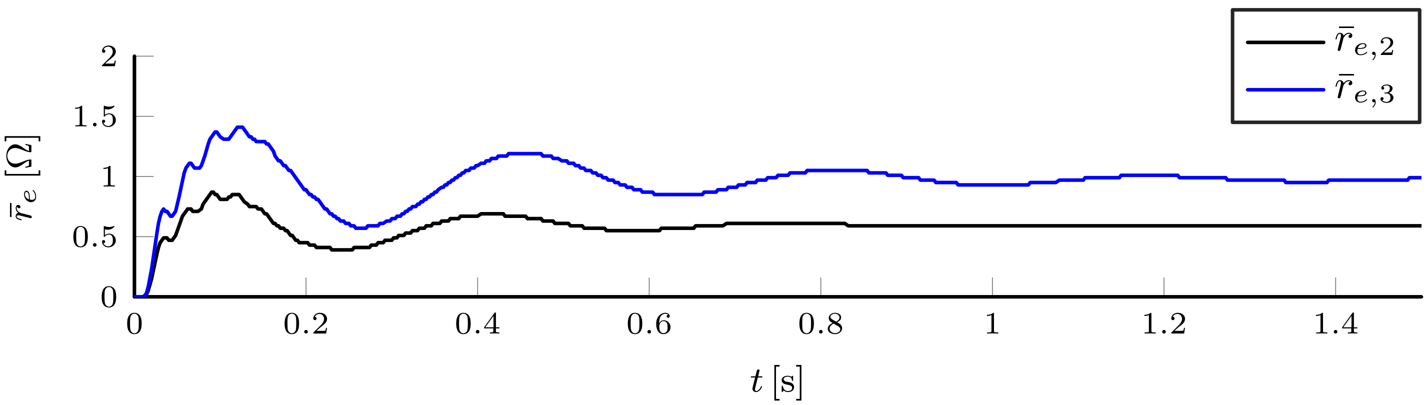


Figure 17: External resistances.

## Indirect Field-Oriented Control

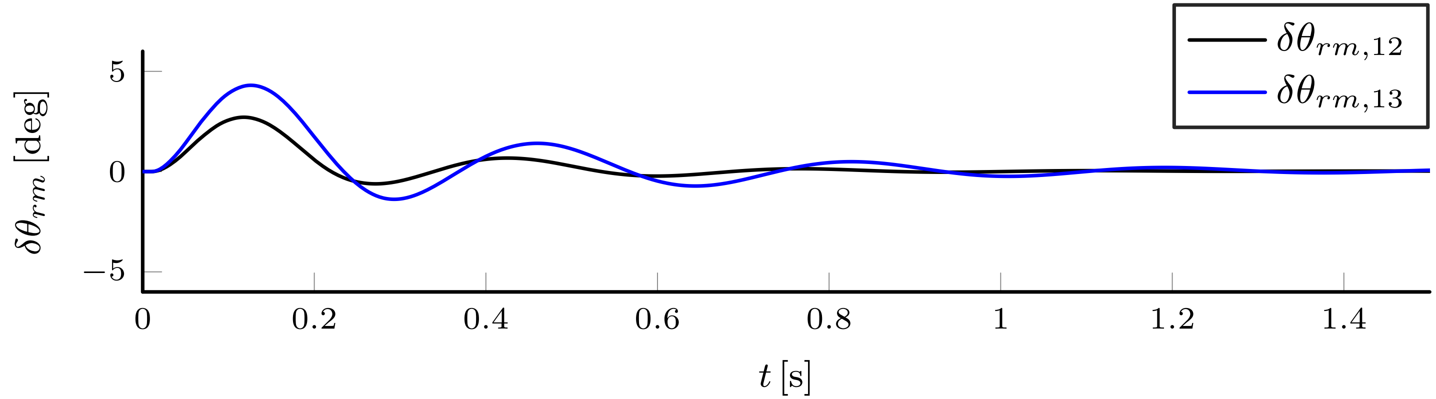


Figure 18: Rotor position errors.

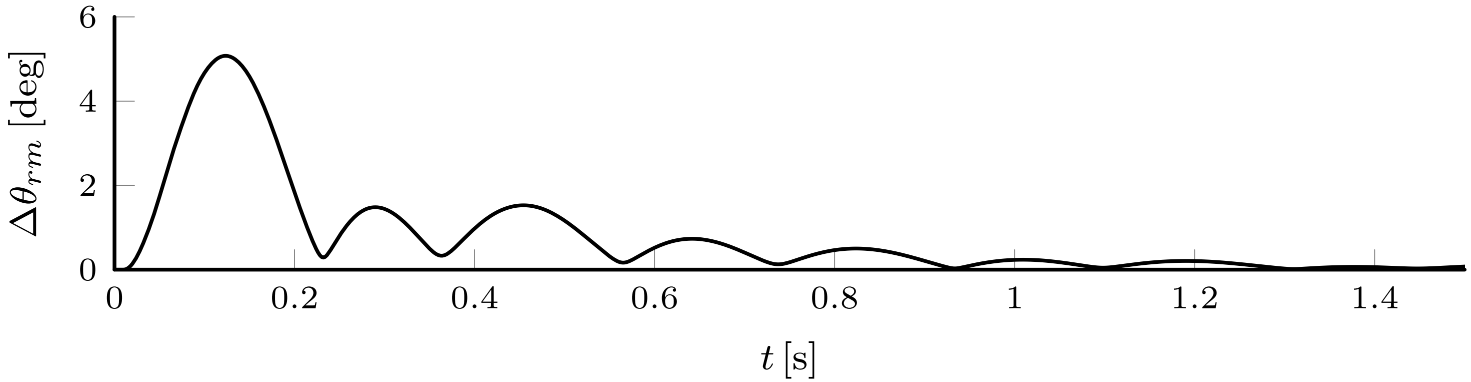


Figure 19: Normed position error.

**Comparison between PI non-optimal controller and $\mathcal{H}_\infty$ controller (CVHz)**

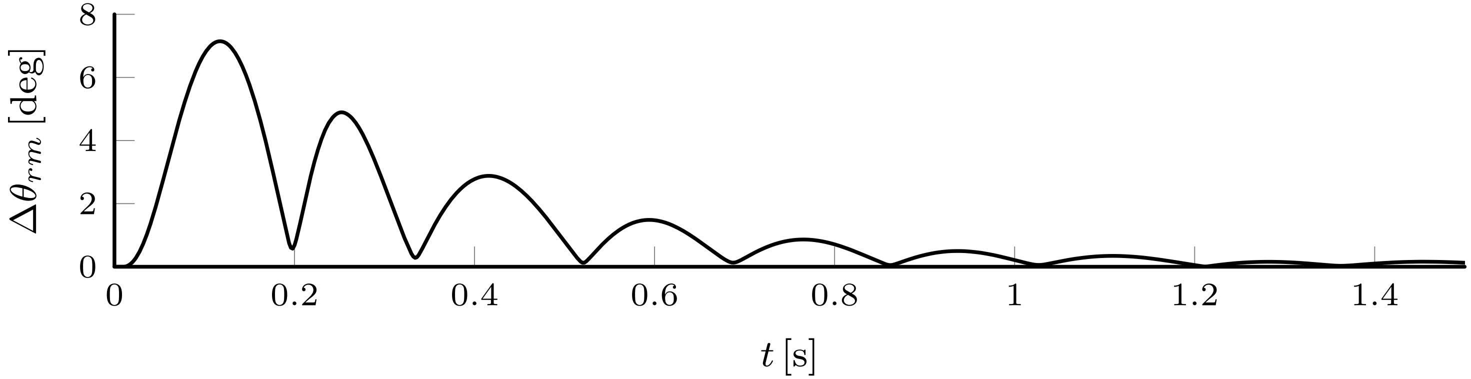


Figure 20: Normed position error; optimal control.

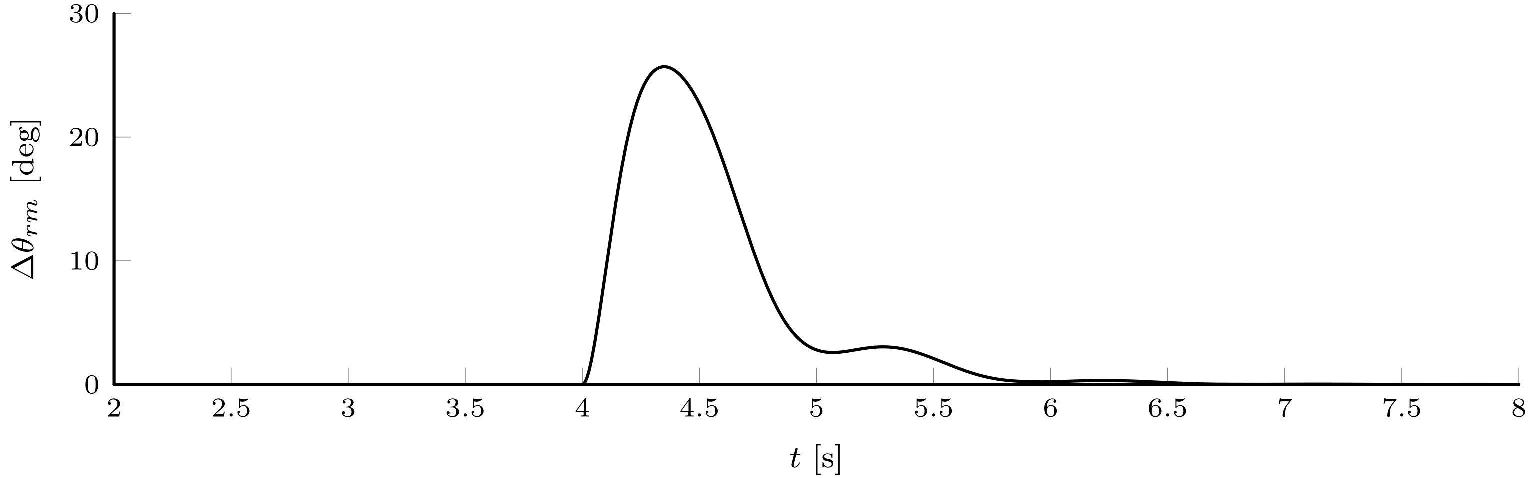


Figure 21: Normed position error; PI non-optimal control [2].

**Comparison between PI non-optimal controller and $\mathcal{H}_\infty$ controller (IDFOC)**

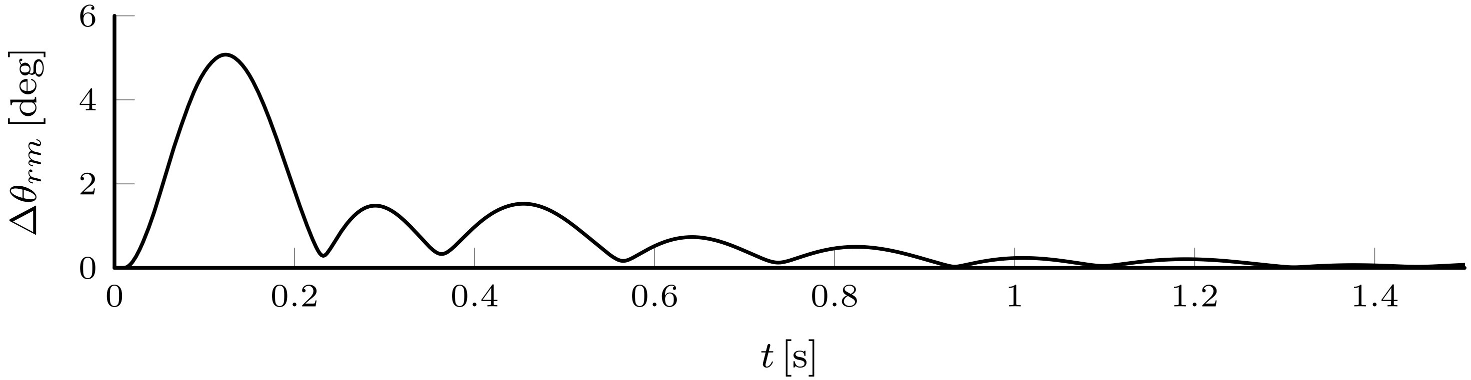


Figure 22: Normed position error; optimal control.

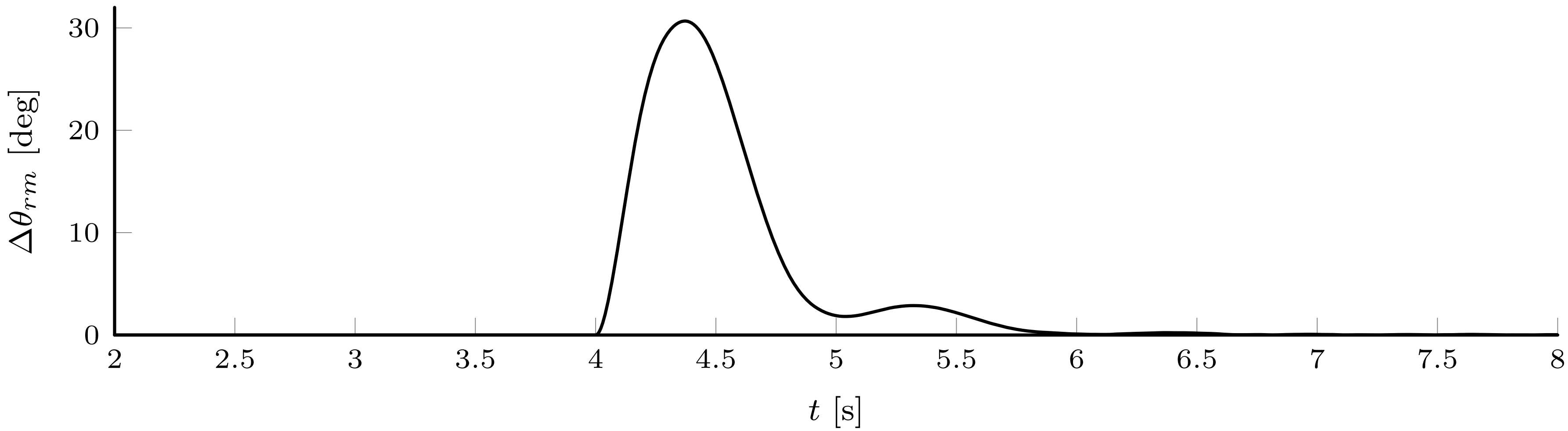


Figure 23: Normed position error; PI non-optimal control [2].

**Comparison Summary**

| | Optimal Control | | Standard PI | |
|---|---|---|---|---|
| | CVHz | IDFOC | CVHz | IDFOC |
| **Peak error** [deg] | 7.1 | 5.1 | 25.7 | 30.7 |
| **Settling time** [s] | 1.15 | 0.88 | 2.39 | 1.89 |

# Conclusions

**Summary**

- Linearization of the IM model
- Optimal control design for rotor position synchronization in CCMM configuration.
- Numerical simulations:
    - Optimal controller was superior to standard PI control
    - IDFOC was superior than CVHz
- Initial results are promising
- Higher complexity of the design and of the controller itself

**Future Work**

- Experimental validation currently underway using a new aerospace actuation testbed at CSU
- Explore alternative synchronization methods with higher energy efficiency (energy recovery)

**Thank you! Any questions?**

# References I


A. Debiane, J. Daclat, R. Denis, G. Dauphin-Tanguy, and J. Mare, "Presage: Virtual testing platform application to thrust reverser actuation system," in *3rd International Conference on Systems and Control.* IEEE, 2013, pp. 1127–1133.

C. d. A. Lima, J. Cale, and K. E. Shahroudi, "Rotor position synchronization in central-converter multi-motor electric actuation systems," *Energies*, vol. 14, no. 22, 2021. [Online]. Available: https://www.mdpi.com/1996-1073/14/22/7485